Title
Classification of Decompensated Heart Failure From Clinical and Home Ballistocardiography

Journal
IEEE Transactions on Biomedical Engineering, 67(5)

ISSN
0018-9294

Authors
Aydemir, Varol Burak
Nagesh, Supriya
Shandhi, Mobashir Hasan
et al.

Publication Date
2020-05-01

DOI
10.1109/tbme.2019.2935619

Peer reviewed

HHS Public Access

Author manuscript

IEEE Trans Biomed Eng. Author manuscript; available in PMC 2021 May 01.

Published in final edited form as:

IEEE Trans Biomed Eng. 2020 May ; 67(5): 1303–1313. doi:10.1109/TBME.2019.2935619.

Classification of Decompensated Heart Failure from Clinical and Home Ballistocardiography

V. Burak Aydemir,
School of Electrical and Computer Engineering, Georgia Institute of Technology, Atlanta, GA, USA

Supriya Nagesh,
School of Electrical and Computer Engineering, Georgia Institute of Technology, Atlanta, GA, USA

Md Mobashir Hasan Shandhi [Student Member, IEEE],
School of Electrical and Computer Engineering, Georgia Institute of Technology, Atlanta, GA, USA

Joanna Fan,
Department of Medicine, University of California, San Francisco, CA, USA

Liviu Klein,
Department of Medicine, University of California, San Francisco, CA, USA

Mozziyar Etemadi,
Department of Anesthesiology and Department of Biomedical Engineering, Northwestern University, Chicago, IL, USA

J. Alex Heller,
Department of Anesthesiology and Department of Biomedical Engineering, Northwestern University, Chicago, IL, USA

Omer T. Inan [Senior Member, IEEE],
School of Electrical and Computer Engineering, Georgia Institute of Technology, Atlanta, GA, USA

James M. Rehg [Member, IEEE]
School of Interactive Computing, Georgia Institute of Technology, Atlanta, GA, USA

Abstract

Objective—To improve home monitoring of heart failure patients so as to reduce emergency room visits and hospital readmissions. We aim to do this by analyzing the ballistocardiogram (BCG) to evaluate the clinical state of the patient.

Corresponding author: v.burakaydemir@gatech.edu.

Disclosure

Omer T. Inan is a Scentific Advisor to Physiowave, Inc., a manufacturer of ballistocardiogram measurement weighing scales.

Methods—1) High quality BCG signals were collected at home from HF patients after discharge. 2) The BCG recordings were preprocessed to exclude outliers and artifacts. 3) Parameters of the BCG that contain information about the cardiovascular system were extracted. These features were used for the task of classification of the BCG recording based on the status of HF.

Results—The best AUC score for the task of classification obtained was 0.78 using slight variant of the leave one subject out validation method.

Conclusion—This work demonstrates that high quality BCG signals can be collected in a home environment and used to detect the clinical state of HF patients.

Significance—In future work, a clinician/caregiver can be introduced into the system so that appropriate interventions can be performed based on the clinical state monitored at home.

Keywords

Ballistocardiography; Machine Learning; Heart Failure

I. Introduction

Heart failure (HF) is a progressive condition in which the heart is not able to pump enough blood to meet the body's demands. Between 2011 and 2014, 6.5 million American adults were diagnosed with HF, with 670,000 patients diagnosed annually. Estimates for 2030 suggest that the number of adults with HF could exceed 8 million. Patients with chronic compensated HF are at risk for a transition to acute decompensated HF, in which increasing pulmonary congestion leads to hospitalization [1]. Patients who have been hospitalized for HF have a higher risk of rehospitalization and mortality, and this risk increases with each repeated hospitalization [2]. For Medicare patients alone, the 30 day readmission rate is 33.3% [3] and the cost of HF-related readmissions is a primary cost-driver in the US healthcare system.

As a consequence of the high public health costs associated with HF readmission, there has been a focus on developing methods for monitoring HF patients to identify the risk of decompensation, so that interventions can be deployed to reduce rehospitalization and improve patient outcomes. Unfortunately, the standard approach of monitoring patients at periodic outpatient visits is not sufficient to reduce the occurrence of urgent hospitalization [4]. A substantial amount of work has focused on monitoring *patient symptoms* which are correlated with rehospitalization [5]. For example, gradual weight gain is a known risk factor [6], and several studies investigated daily weight monitoring as a means to predict readmission risk [7], [8]. However, these studies and others [9] have demonstrated that using weight pattern as a predictor results in high false positive rates.

While monitoring patient symptomatology does not appear to be an effective way to reduce hospitalization, there is evidence that *physiological measures* of cardio-pulmonary function can yield effective predictors. It has been shown that decompensation is frequently associated with increased pulmonary and intracardiac pressure, which can manifest days or weeks before patient-reported symptoms emerge [10], [11]. In [12], it was demonstrated that using a wireless implantable hemodynamic sensor to obtain daily measurements of

pulmonary artery pressure resulted in a 37% reduction in HF-related hospitalizations in the treatment group when compared to a control group that only received the standard of care. At present, the implantable hemodynamic monitoring approach is the only method that has demonstrated significant improvement in readmission outcomes in a randomized controlled trial. Additional converging evidence that physiological measures can improve the prediction of HF events is provided by the multiSENSE observational study [13]. In this study of HF patients who received CRT-D device for treatment, a combination of heart rate, respiratory rate, activity, bioimpedance and heart sounds were shown to be effective in predicting HF events. However, the reliance of [12] and [13] on implantable sensors results in significant expense and limits their applicability to only a subset of HF patients.

A significant body of work has explored *noninvasive* physiological monitoring as a means to predict readmission risk. One example is the observational MUSIC study [14], which utilized the same sensing modalities as multiSENSE [13] (with the exception of heart sounds). They achieved 63% sensitivity and 92% specificity in detecting HF events. In another example, Packer et al. assessed the utility of impedance cardiography (ICG) in predicting the deteriorating state of HF patients [15]. Three ICG parameters (velocity index, thoracic fluid content index, and left ventricular ejection time) were shown to be useful in predicting a HF event within a two week interval. While these approaches produced promising results, they require participants to wear a device which makes continuous contact with the skin, leading to a high amount of participant burden.

Among the noninvasive methods, several studies have explored the use of *non-contact* radio-wave (RF-based) sensors for monitoring cardiopulmonary function. An overview of the approach can be found in [16], which presents *EasySense*, a novel system for tracking heart motion using ultra-wide band radar. EasySense combines a transmitter and receiver in a single device, to be worn on or near the chest, making it convenient to deploy. It is currently being evaluated for use with HF patients. A related approach for monitoring fluid build-up in the lungs, which is a risk marker for decompensation, is the Remote Dielectric Sensing (ReDS™) technology proposed in [17] and validated in [18]. The authors show that there is a high correlation between the ReDS™ sensor and the gold standard of chest computed tomography in measuring the quantity of fluid in patients with and without acute heart failure. Using this technology to guide therapy was shown in [19] to result in a significant decrease in HF-related re-hospitalizations. In the ReDS™ approach, the transmitter and receiver are embedded in a vest which can be worn on top of clothing, and are positioned on opposite sides of the torso. While this provides flexibility, it is cumbersome to have to put on and take off a vest which is tethered to monitoring equipment every time a reading is required.

In contrast, the RF-based approach to sleep monitoring described in [4] uses a bedside device to continuously and passively monitor nocturnal respiration in order to detect events of decompensation. While this approach is low burden, it is limited to monitoring during sleep. Note that all RF-based approaches can be sensitive to the location of the transmitter-receiver pair relative to the body and can suffer from multipath effects and other sources of noise. While these prior works are promising, no current method has emerged as a clear alternative to implantable monitors. Furthermore, it should be noted that any noninvasive

approaches which require patient interaction on an on-going basis will face additional compliance issues [20].

In this work, we present a non-invasive, cost-effective, low burden, and easily deployable approach to remote monitoring of HF patients using ballistocardiogram (BCG) signals collected in the home environment. BCG is a measurement of the heart's mechanical forces in reaction to the process of the ejection of blood [21]–[26]. Reaction force measurements can be obtained with a variety of sensing approaches, including a modified weighing scale [27], a wearable accelerometer [28], a wearable camera [29] and a toilet seat [30],[31]. All BCG devices currently require active participation from the user. Both the scale and toilet seat methods for recording BCG have the advantage of integrating the sensing task into appliances that are already in routine use in the home. However, both sensing approaches require additional accommodation by the user which could be burdensome. In the case of the toilet sensor, the user is not allowed to actually use the toilet during the time when the data is acquired. In the case of the weighing scale, the user must additionally hold onto a handle which is used to acquire the ECG signal. Thus the question of which BCG approach will lead to highest adherence is currently open.

BCG measurements obtained from a weighing scale have been shown to be strongly-correlated with cardiac output [27] and to contain usable information about the state of decompensation in HF. In [32], a single BCG feature (RMS power) was shown to reveal changes in clinical state in 10 decompensated HF patients. In addition, a wearable seismocargiography (SCG) sensor, consisting of a 3-axis accelerometer, was used in [28] to collect data from an inpatient population during a six minute walk test. This work showed that machine learning techniques can assess the state of HF in an inpatient setting by analyzing the cardiac response to exercise contained in the SCG signal. In contrast, the current paper demonstrates the ability to classify compensated vs. decompensated HF status by analyzing *outpatient BCG data* collected at home.

Our long term goal is to be able to predict the future risk of an event of decompensation from signals collected at home, in order to inform careproviders and prevent readmission, as illustrated in Fig. 1. There are two challenges in achieving this goal. First, we must establish that BCG signals collected by participants at home have sufficient data quality and reliability to support the classification of compensated and decompensated states. Second, we must demonstrate that home-collected BCG can serve as a predictor for future decompensation risk. This paper addresses the first challenge of analyzing in-home BCG recordings to distinguish compensation from decompensation. It can be viewed as a feasibility study to identify the features of BCG that are useful in classifying HF state. Having established the feasibility of HF status classification from BCG (see Sec. IV), the next step will be to investigate the prediction of future decompensation risk.

In this study, we show that features derived from BCG waveforms can be used in a machine learning framework to classify between compensated and decompensated heart failure in the outpatient setting. We present an analysis of the most effective predictive features and report classification results with an Area Under the ROC (AUC) of 0.78. This promising finding points towards the potential of BCG to define an effective risk index for intervention in HF

to prevent readmission. We believe this is the first study to investigate the utility of BCG signals at home in the HF domain.

The paper is organized as follows: Section II describes our study population and sensing hardware. Section III describes our approach to signal processing, feature extraction, and classifier design. Section IV presents our experimental results for classifying decompensation. Section V provides a discussion of our findings and potential future work.

II. Materials

A. Data collection and experimental protocol

The study was conducted under a protocol reviewed and approved by the University of California, San Francisco (UCSF) Institutional Review Board and the Georgia Institute of Technology Institutional Review Board. A total of 43 subjects (6 females and 37 males), with heart failure participated in the study (Age: 59.1 ± 12.7 years, Height: 177.5 ± 10.4 cm). Inclusion criteria was patients with heart failure. The only exclusion criteria for the study was if the patient was hospice-bound or has dementia. Note that the number of female participants is currently small in this preliminary study. Data collection is on-going and we expect our sample to become more balanced over time. Additionally, 40 of our subjects had heart failure with reduced ejection fraction and the remaining subjects had heart failure with preserved ejection fraction. The presentation of acute decompensation in the two groups would share many properties in common [33], [34]. Hence we did not perform separate analyses for these groups. All subjects provided written, informed consent before experimentation. More details regarding the subjects are presented in Table I.

The purpose of the protocol was to observe the correlation between longitudinal hemodynamic changes in the subjects and their clinical status (i.e., decompensated and compensated states). Our data collection approach is based on our prior work [35], which demonstrated the feasibility of simultaneous at-home recording of BCG and electrocardiogram (ECG) signals using a modified bathroom weighing scale. BCG and ECG signals were simultaneously recorded using a previously-validated modified weighing scale [23]. The BCG signals were collected from subject populations under two conditions: *clinic* and *home*. The clinic condition includes all inpatient recordings, which were obtained from patients who were hospitalized for acute decompensation. BCG readings were obtained soon after admission and during the period of hospitalization until discharge. These signals include both decompensated examples and compensated BCG signals collected a few days prior to discharge. This condition also includes a small number of outpatients whose BCG signals were recorded during follow-up visits to the clinic. The home condition corresponded to patients who took daily BCG readings at home for 30 days. Section III and Figure 4 provide a detailed description of the organization of these recordings into datasets for our experiments.

During data collection, each subject was asked to stand still on the scale for 30 seconds while holding the handlebar as shown in Figure 1. Three to four consecutive recordings were collected to ensure data reliability for inpatient recordings. At home subjects take two consecutive recordings per day. The ground truth clinical status was determined in the

following manner: In the case of recordings obtained at home, the subjects are considered to be in the compensated state. The evidence for this decision is two-fold: First, there were no rehospitalizations for the subjects following discharge. Second, we followed-up with each subject periodically by phone, which provided an additional check. For the recordings obtained at the hospital (either inpatient or outpatient), the clinical status – i.e., decompensated versus compensated – was determined by the physician based on vital signs (e.g., blood pressure and heart rate), physical exam findings (e.g., jugular venous pressure), and symptoms (e.g., shortness of breath), as described in detail in prior work [28]. These gold standard assessments of HF status are then used as labels in the supervised machine learning approaches described in Sec. III.

B. Sensing Hardware

BCG was measured using a previously-validated modified weighing scale. The modified weighing scale (BC534, Tanita, Tokyo, Japan) was developed in previous work using an analog amplifier and strain gauge bridge [23]. The ECG signal was measured simultaneously with handlebar electrodes interfaced to custom electronics [36]. Data was recorded using a SD card in the scale, and later accessed by a computer. The sampling frequency for ECG and BCG are 1kHz and 125Hz, respectively. In our analysis, BCG is upsampled to 1kHz.

III. Methods

We now describe the method used to classify a single BCG recording to obtain a classification of compensated or decompensated. This process is illustrated in Fig. 2. The first step is preprocessing of the BCG and ECG signals and the segmentation of the BCG signal into individual beats. This is followed by averaging and feature extraction from BCG. The final step is classification using the extracted BCG features.

A. BCG Signal Preprocessing

The collected BCG and ECG signals are first preprocessed to remove noisy and unreliable recordings. The first step is to crop the first 5 seconds from each recording. This initial part of the signal can contain instabilities in the BCG while the subject is reaching a steady state on the weighing scale. Both the signals are then bandpass filtered to magnify the spectral region of interest. A passband range of 3–25 Hz is used to amplify the R-peaks in the ECG signals, with an equiripple FIR filter of order 903, while a passband range of 2–10Hz was chosen for the BCG signals, with equiripple FIR filter of order 1468, after a visual inspection of the filtered signals. MATLAB's designfilt function implemented the filter with 1kHz sampling rate.

The next step in processing is to segment the BCG recording into separate beats. This is achieved by detecting the R-peaks in the corresponding ECG signal. Two different algorithms were used for R-peak detection; Pan-Tompkins [37] and Phasor Transform [38]. In the case of the Pan-Tompkins algorithm, an implementation by Physionet [39] is used, and in the case of the Phasor Transform algorithm, a custom implementation by the authors of this paper is used. Peaks that were not detected by both the algorithms were discarded so

as to ensure fewer false positives in the peak detection process. As an additional measure to ensure proper detection, the ECG signal is segmented into 6 second intervals and analyzed for R-peaks. In the case where an R-peak cannot be detected reliably in two or more consecutive segments, the recording is discarded. The ratio of discarded to total number of recordings is 0.096. This is to ensure that we minimize the number of incorrectly segmented beats because of undetected or misdetected R-peaks. Using the obtained R-peak locations, the BCG signal is then segmented into beats and arranged as a beat array BCG as shown in panel (b) of Figure 2.

$$BCG = \left\{ b^1[t], b^2[t], \cdots, b^N[t] \right\} \tag{1}$$

where $b^i[t]$ is the i^{th} BCG beat, and $t = 1, 2, \cdots, T$ where T is the mean RR interval length.

It is reasonable to expect that some of the beats in the beat array may contain motion artifacts that overpower the cardiovascular information in the signal. We eliminate beats that seem to be outliers [40] according to the following rule:

$$\begin{cases} \dfrac{\left\| \left| e[t] - b^i[t] \right| \geq \alpha\sigma[t] \right\|_0}{T} > \dfrac{\beta}{100}; & b^i[t] \text{ is eliminated} \\ \text{otherwise}; & b^i[t] \text{ is kept} \end{cases} \tag{2}$$

where,

$$e[t] = \frac{1}{N} \sum_{i=1}^{N} b^i[t],$$

$$\sigma[t] = \sqrt{\frac{1}{N-1} \sum_{i=1}^{N} \left(b^i[t] - e[t] \right)^2}, \tag{3}$$
$$0 < \alpha < \infty, 0 < \beta < 100.$$

$e[t]$ is also called ensemble averaged beat. This rule eliminates those beats whose β% of samples are α standard deviations away from the ensemble averaged beat. In our implementation, we perform this elimination twice with $(\alpha, \beta) = \{(3, 2), (1, 25)\}$. These values are tuned such that the resulting ensemble averaged beat after elimination has a visually-similar morphology to reference examples in the literature [41].

The signal quality is assessed using the maximum likelihood estimate of the signal to noise ratio (SNR_{ML}) [23] using sub-ensemble averaging. The procedure for computing this metric is as follows. First, the BCG beat array, defined as in equation 1, is segmented into groups of 5 beats. The sub-ensemble average beat is obtained by computing the mean of the beats in every group. This is represented by the sub-ensemble average matrix S:

$$S = [s_1 \; s_2 \cdots s_M], \tag{4}$$

where s_j is the average of the j^{th} group of beats. Next, the maximum likelihood estimate of the SNR between the i^{th} and j^{th} sub-ensemble average is computed as follows:

$$SNR_{ij} = \frac{2\langle s_i, s_j \rangle}{\|s_i - s_j\|^2}, \tag{5}$$

where $\langle s_i, s_j \rangle = s_i^\top s_j$ is the standard inner product and $\| \cdot \|$ is the corresponding norm.

Finally, the overall SNR for the subject is obtained by averaging the SNR values over all distinct sub-ensemble pairs:

$$SNR_{ML} = \underset{j > i}{\text{avg}}\left(SNR_{ij}\right). \tag{6}$$

Figure 3 shows an example of two recordings - the plot in red is a low-quality waveform and the one in blue is a high-quality waveform obtained at home.

B. Feature Extraction

Various features computed from the BCG signal have been explored in previous work related to monitoring cardiac activity. In [42], the authors track the cardiac time intervals using temporal features within a BCG beat. In [43], the authors use wavelet features to estimate the heart rate from unsegmented BCG signals. In [44], statistics of both temporal and spectral features are extracted for the purpose of detecting Atrial Fibrillation from BCG signals. We follow a similar approach of extracting the statistics of temporal features in the BCG signal. We utilize the standard features used in the case of BCG signals [45], along with additional L1 and L2 norm-based features. Altogether, we utilize three types of features: Ensemble Averaged Beat, Waveform Consistency and Miscellaneous features.

1) Ensemble Averaged Beat Features—Ensemble averaged beat features have been shown in the past to correlate with cardiovascular parameters such as pre-ejection period and cardiac output [46] [47]. We include these features in our analysis as these cardiovascular parameters could be informative about the status of the patient. Table II shows the features extracted from the ensemble averaged beat.

2) Waveform Consistency Features—In [48], it is shown that a signal consistency metric could be a useful feature for monitoring the status of a HF patient. We extracted 28 features that quantify the consistency of the BCG signal. Initially, the BCG beat array is divided into four equal sized sub-beat arrays. From these sub-beat arrays, sub-ensemble averages are computed. Waveform consistency features are computed using the sub-ensemble and ensemble average beats. The subensemble features can capture the changes in consistency of the waveform over the course of the recording while still providing some noise reduction benefit. The complete set of waveform consistency features can be seen in Table III.

3) Miscellaneous Features—There are other features computed that do not strictly fall into the other two feature classes, but could contain information about the patient's state. For

example, weight is one of the metrics used in the current standard of care. The other features listed in Table IV target the information in the beat to beat variations in the BCG.

C. Classifier Design

We now describe the design of the classifier which maps a vector of 48 features extracted from a single BCG recording (see Sec. III-B) into an output of compensated vs. decompensated state. This is a supervised binary classification problem. We explored three different classifier architectures for this task: multilayer perceptron, support vector machine, and random forest. These classifiers output a confidence score corresponding to the probability that a feature vector belongs to the positive class of decompensated HF. For each classifier, feature vectors are normalized using z-score from the training set. There are two steps in training the classifier: 1) Determining the hyperparameters (optimizing the classifier design); and 2) Training the network parameters (optimizing the classifier weights). We now explain these steps in more detail for each of our chosen architectures:

1) Multilayer perceptron—A multilayer perceptron (MLP) is a feed-forward architecture composed of layers of computational units called neurons. Each unit receives a weighted input vector and passes along a non-linear function of that information to the neurons in the next layer. The output layer is designed to have one neuron that computes the probability of the recording belonging to the decompensated state. For our implementation, we optimize the number of layers and neurons per layer as hyperparameters. We use cross-entropy loss and conjugate-gradient descent for training the network weights.

2) Support Vector Machine—A support vector machine (SVM) finds the best decision hyperplane separating the two classes in a high-dimensional feature space. In its simplest form, the linear SVM tries to find a maximum margin separating hyperplane in the feature set. By using different kernels for feature mapping, non-linear decision boundaries can be attained. In our implementation, we used the linear, polynomial, and RBF kernels and tune the hyperparameters associated with these kernels.

3) Random Forest—A random forest (RF) is a combination of decision trees where each decision tree is trained on a resampled training set. Each decision tree is a classifier, with a tree structure. From each node of the tree, a different child node is reached based on the value of one of the features. When it gets to the last level of nodes, a decision is made about the class. Classifications from the different decision trees can be treated as a classification score. The more the decision trees votes in favor of a particular class, more confident the random forest decision is. In our implementation, the number of decision trees and split criterion in each node are optimized.

Apart from classification into compensated and decompensated HF, we also investigate the importance of different features in performing the above task. Feature ranking helps us identify relevant features. In our work, we use the linear SVM weights for feature ranking [49]. A linear SVM is trained on the data to obtain the weights w corresponding to the features. The value of $|w_j|$ is directly proportional to the importance of the j^{th} feature in decision making. In our implementation, we rank the features based on the value of w_j^2.

We further investigate the importance of the top five features. We can identify their individual contributions to the task of classification into compensated and decompensated HF as follows: We remove each feature one at a time from the data set and determine the AUC score using the best performing classifier.

IV. Experimental Results

We performed two sets of experiments to analyze the effectiveness of BCG signals for discriminating between compensated and decompensated states. The experiment design is described in Section IV-A, and our experimental findings are described in Sections IV-B and IV-C.

A. Experiment Designs

The dataset construction for the experiments is illustrated in Figure 4. In this diagram, the white boxes identify exclusion criteria by which recordings are removed from the total available set in order to construct a specific dataset of interest. The first set of experiments has three parts: classification, feature importance ranking, and feature ablation. It is described in Section III. These experiments utilize all valid recordings from 43 subjects (Dataset 1). They test the overall effectiveness of the BCG classifier and identify the most important BCG features. The second set of experiments, described in Section IV-C, examine the effect of the recording condition (home vs. clinic) on the accuracy of the BCG classifier.

Dataset 2 is constructed in order to measure the accuracy of the classifier in predicting compensation state using data collected at home. In order to obtain the Dataset 2, we removed 156 compensated clinic recordings (from cell (C, CI) in the table corresponding to Dataset 1 in Figure 4). As described in Section II, all recordings in the home condition came from compensated patients. In order to obtain a balanced training and testing set, we kept all 311 decompensated clinic recordings (cell (D, CI)) from the Dataset 1. Dataset 3 consists of all recordings collected in the clinic. It combines all inpatient recordings with the outpatients (55 compensated and 4 decompensated) who had clinical recordings at clinic visits.

We use a variation of Leave One Subject Out (LOSO) cross-validation to predict the generalization performance of the classifier in all experiments. In standard LOSO cross validation, the model is trained on the data from all the subjects except one, and the held-out subject is then used as the test data. This process is repeated so as to test on all subjects. In our dataset, some subjects contain data belonging to only one class. For example, a subject with only one day of inpatient recording may have only decompensated recordings. And similarly, a subject with only one day of outpatient recording will have only compensated recordings. To overcome this problem, we combine together multiple subjects who have data belonging to only one class. For example, in Dataset 1 there were 13 subjects who had only compensated recordings and (by coincidence) another 13 subjects with only decompensated recordings. We paired these subjects at random to construct 13 ”virtual” subjects containing data from each class for the LOSO procedure. The receiver operating characteristics (ROC) curve and the corresponding area under the curve (AUC) value are computed for each classifier. For each classifier, we obtain confidence scores for each of the validation set

recordings in each of the cross-validation splits. We form the ROC curve for each classifier from the complete set of these confidences.

B. Classifier Performance and Feature Analysis

The goals of the experiments in this section are to identify the most effective classification architecture for predicting decompensation from BCG, and to analyze the BCG features to determine which features are most effective for the prediction task.

We train five different classifiers: random forest, linear SVM, polynomial SVM, RBF SVM, and MLP, using Dataset 1 (see Figure 4). We perform LOSO cross-validation with 30 folds, and obtain the AUC values for each classifier reported in Table V. We see that the SVM with RBF kernel performs the best among the different classifiers used. The ROC curve corresponding to RBF SVM is shown in Figure 5.

Our next goal was to analyze the contribution of individual features to the classification performance and to identify the most important features. The first step was to train a linear SVM as described in Sec. III, and rank the features based on the SVM weights. The ten most important features are shown in Figure 6, in the order of decreasing importance. We note that the three global mean and median features appear to be significantly more informative than the others. However, using a linear kernel in an SVM results in a linear classifier, so this analysis should be viewed as a first step in understanding feature importance. Of course if the dataset was linearly separable, then this classifier would yield the optimal performance, but we know from Table V that this is not the case. Moreover, the mean and median features are likely to be correlated, which will make it difficult to tease apart their contributions using a linear model.

In order to obtain a more accurate assessment of the importance of the top-ranked features, we performed an additional study in which we dropped features one at a time and trained an SVM with an RBF kernel on the remaining features. The drop in accuracy that results from omitting one feature is a measure of that feature's importance. Since an RBF SVM is capable of learning nonlinear decision boundaries, this analysis can provide a more nuanced picture of feature importance at an increased computational cost. Table VI shows the results of this analysis applied to the top-five features from Figure 6. We see that *globmean2* is the most important feature under this analysis, followed by *RJ/RR*. The remaining features are of roughly equal importance.

C. Classification of Decompensation in Clinic and Home Settings

The purpose of the experiments in this section is to investigate whether there is a performance difference between two settings: home and clinic. For each setting, AUC is computed using the corresponding dataset. Results can be seen in Table VII. We see that the AUC score obtained is higher in the home setting.

Finally, we examine the measurement yield reflecting the device usage from the users of this study. We quantify it with the following equation:

$$\text{Measurement Yield} = \frac{\text{Total \# of recordings}}{\text{Total \# of recordings supposed to be received according to the protocol.}} \quad (7)$$

Measurement yield in our dataset under the home condition is 0.80. It should be noted that some subjects had other medical conditions, e.g. orthopedic leg injury, that prevented them from consistently recording data.

V. Discussion

We performed two studies to identify the most important BCG features for classification. Analysis of the weights in a linear SVM was used to identify the top 10 features (Figure 6), and leave-one-feature out analysis with RBF SVM identified the contribution of each of these features to the overall accuracy (Table VI). These two analyses provide converging evidence for the importance of global mean features, as *globmean1* was the top-ranked feature under the linear model, and *globmean2* was found to have the greatest impact on the accuracy of the RBF SVM. Moreover, the fact that the RJ/RR feature was ranked second in importance under the RBF SVM suggests that the non-linear RBF classifier can obtain information from this feature which is not present in the (likely highly-correlated) global mean type features. These analyses suggest that global mean and RJ/RR features provide valuable and complementary information for classification. It is interesting to note that the patient's weight was not included within the ten important features under the linear model, implying BCG features are more informative than weight alone. Moreover, when weight is removed from the feature set for the RBF SVM, the AUC performance decreases by only 0.04, suggesting that weight is of limited value when combined with BCG features.

Additional information about feature importance can be obtained by visualizing the class-conditional feature distributions, as illustrated in Figure 7. The figure gives the histograms of the values of the ten features from Figure 6, for both the compensated and decompensated class, using Dataset 1. The first observation we can make from the plots is that there is a significant overlap between the compensated and decompensated distributions. This reinforces the difficulty of the classification task, the need for considering multiple features, and the importance of utilizing a non-linear classifier such as the RBF SVM. Additional challenges stem from the fact that we are considering 30s intervals of the BCG signals, and therefore lack long-term temporal context and the ability to adapt the model to individual participants. It is interesting to note that in the case of most features, the distribution of the decompensated class is shifted slightly to the right. This can be seen from their mean values, shown as dotted lines.

We conducted an analysis to identify the impact of the recording setting (home vs. clinic) on the classifier performance. A primary concern is whether home recordings, which take place without the supervision of clincal personnel, would exhibit a decrease in classification accuracy. The results from Table VII show that the recordings collected at home, without supervision by clinicians, are equally good at capturing the information required for classification of the clinical state of HF. Specifically, we see that Datasets 2 and 3 (in Figure

4) use identical sets of decompensated clinic recordings. The major difference between these datasets is that Dataset 2 uses 797 compensated recordings from the home setting, while Dataset 3 uses 156 compensated recordings from the clinic setting. If there were issues of signal quality in the data collected at home (without the benefit of clinical supervision), we might expect degredation in the classifier performance. In fact, we find that the AUC is 6% higher in the home setting. We believe the increase can be attributed to the fact that we have approximately two times more recordings in the home setting, which allows the classifier to learn a more accurate model of the concept class.

Furthermore, the measurement yield of 0.8 in the home condition (see Section IV-C) is an encouraging finding from the perspective of the adoption and use of the measurement scale by HF populations. This is an important validation step for the future scenario of using home-collected data to trigger and tailor interventions.

In summary, we believe our findings are encouraging for the potential use of the BCG signal to detect, and eventually predict, states of decompensation based on data collected at home. One caveat is that we have not collected data from decompensated participants at home. However, there is little reason to believe the presentation of acute decompensation would differ in the home condition vs. the clinical condition (i.e. at admission time), given that there do not appear to be any substantial quality issues with home-collected data. It should also be noted that the low number of female participants is a potential limitation of our findings. The next step in advancing towards the prediction of decompensation risk will be to study the deviation of BCG features over time relative to baseline, for outpatient participants that are becoming decompensated.

VI. Conclusion

This work is the first to successfully record BCG signals from compensated participants in a home environment, and to demonstrate that compensated and decompensated states of HF can be distinguished using machine learning analysis of the BCG waveform. By comparing classifier performance on data collected in home and clinical settings, we demonstrate that home-collected data is comparable in quality to the clinical setting. The methods presented in this paper open the door to a new approach to home monitoring of patients. We hypothesize that the analysis of home-collected BCG signals, when paired with proper feedback and intervention by clinicians, could ultimately lead to a reduction in the number of hospital readmissions, in their associated morbidity and cost, and eventually to an improvement in the quality of life for patients after discharge.

Acknowledgments

Research reported in this publication was supported, in part, by the National Heart, Lung and Blood Institute under R01HL130619. The content is solely the responsibility of the authors and does not necessarily represent the official views of the National Institutes of Health.

References

[1]. Adamson PB, “Pathophysiology of the transition from chronic compensated and acute decompensated heart failure: new insights from continuous monitoring devices,” Current Heart Failure Reports, vol. 6, no. 4, pp. 287–292, 2009. [PubMed: 19948098]

[2]. Benjamin EJ et al., “Heart disease and stroke statistics–2018 update: a report from the American Heart Association,” Circulation, vol. 137, no. 12, pp. e67–e492, 2018. [PubMed: 29386200]

[3]. Kilgore M et al., “Economic burden of hospitalizations of Medicare beneficiaries with heart failure,” Risk management and healthcare policy, vol. 10, p. 63, 2017. [PubMed: 28546776]

[4]. Javed F et al., “Early warning of acute decompensation in heart failure patients using a noncontact measure of stability index,” IEEE Transactions on Biomedical Engineering, vol. 63, no. 2, pp. 438–448, 2016. [PubMed: 26258931]

[5]. Ong M et al., “Effectiveness of Remote Patient Monitoring After Discharge of Hospitalized Patients With Heart Failure: The Better Effectiveness After Transition – Heart Failure (BEAT-HF) Randomized Clinical Trial.,” The Journal of the American Medical Association, vol. 176, pp. 310–18, 2016.

[6]. Chaudhry SI et al., “Patterns of weight change preceding hospitalization for heart failure,” Circulation, vol. 116, no. 14, pp. 1549–1554, 2007. [PubMed: 17846286]

[7]. Cleland JG et al., “Noninvasive home telemonitoring for patients with heart failure at high risk of recurrent admission and death: the Trans-European Network-Home-Care Management System (TEN-HMS) study,” Journal of the American College of Cardiology, vol. 45, no. 10, pp. 1654–1664, 2005. [PubMed: 15893183]

[8]. Zhang J et al., “Predicting hospitalization due to worsening heart failure using daily weight measurement: analysis of the Trans-European Network-Home-Care Management System (TEN-HMS) study,” European journal of heart failure, vol. 11, no. 4, pp. 420–427, 2009. [PubMed: 19252210]

[9]. Abraham WT et al., “Superior performance of intrathoracic impedance-derived fluid index versus daily weight monitoring in heart failure patients: results of the Fluid Accumulation Status Trial (FAST),” Journal of Cardiac Failure, vol. 15, no. 9, p. 813, 2009.

[10]. Zile M et al., “Transition from chronic compensated to acute decompensated heart failure: pathophysiological insights obtained from continuous monitoring of intracardiac pressures.,” Circulation, vol. 118, pp. 1433–1441, 2008. [PubMed: 18794390]

[11]. Ritzema J et al., “Physician-directed patient self-management of left atrial pressure in advanced chronic heart failure,” Circulation, vol. 121, no. 9, pp. 1086–1095, 2010. [PubMed: 20176990]

[12]. Abraham WT et al., “Wireless pulmonary artery haemodynamic monitoring in chronic heart failure: a randomised controlled trial,” The Lancet, vol. 377, no. 9766, pp. 658–666, 2011.

[13]. Boehmer JP and others., “A Multisensor Algorithm Predicts Heart Failure Events in Patients With Implanted Devices: Results From the MultiSENSE Study,” JACC: Heart Failure, 2017.

[14]. Anand IS et al., “Design and performance of a multisensor heart failure monitoring algorithm: results from the multisensor monitoring in congestive heart failure (MUSIC) study,” Journal of cardiac failure, vol. 18, no. 4, pp. 289–295, 2012. [PubMed: 22464769]

[15]. Packer M et al., “Utility of impedance cardiography for the identification of short-term risk of clinical decompensation in stable patients with chronic heart failure,” Journal of the American College of Cardiology, vol. 47, no. 11, pp. 2245–2252, 2006. [PubMed: 16750691]

[16]. Gao J et al., “A New Direction for Biosensing: RF Sensors for Monitoring Cardio-Pulmonary Function,” in Mobile Health. Rehg Ed et al., pp. 289–312, Springer, 2017.

[17]. Amir O et al., “A novel approach to monitoring pulmonary congestion in heart failure: initial animal and clinical experiences using remote dielectric sensing technology,” Congestive Heart Failure, vol. 19, no. 3, pp. 149–155, 2013. [PubMed: 23350643]

[18]. Amir O et al., “Validation of remote dielectric sensing (ReDS) technology for quantification of lung fluid status: Comparison to high resolution chest computed tomography in patients with and without acute heart failure,” International journal of cardiology, vol. 221, pp. 841–846, 2016. [PubMed: 27434357]

[19]. Amir O et al., “Evaluation of remote dielectric sensing (ReDS) technology-guided therapy for decreasing heart failure rehospitalizations,” International journal of cardiology, vol. 240, pp. 279–284, 2017. [PubMed: 28341372]

[20]. Bhimaraj A, “Remote monitoring of heart failure patients,” Methodist DeBakey cardiovascular journal, vol. 9, no. 1, p. 26, 2013. [PubMed: 23519115]

[21]. Starr I et al., “Studies on the estimation of cardiac ouptut in man, and of abnormalities in cardiac function, from the heart’s recoil and the blood’s impacts; the ballistocardiogram,” American Journal of Physiology-Legacy Content, vol. 127, no. 1, pp. 1–28, 1939.

[22]. Brown HR et al., Clinical ballistocardiography. The Macmillan Company; New York, 1952.

[23]. Inan OT et al., “Robust ballistocardiogram acquisition for home monitoring,” Physiological measurement, vol. 30, no. 2, p. 169, 2009. [PubMed: 19147897]

[24]. Gonzalez-Landaeta R et al., “Heart rate detection from an electronic weighing scale,” Physiological measurement, vol. 29, no. 8, p. 979, 2008. [PubMed: 18641428]

[25]. Gilaberte S. Heart and respiratory rate detection on a bathroom scale based on the ballistocardiogram and the continuous wavelet transform; Engineering in Medicine and Biology Society (EMBC), 2010 Annual International Conference of the IEEE; IEEE; 2010. 2557–2560.

[26]. Shin JH et al., “Non-constrained monitoring of systolic blood pressure on a weighing scale,” Physiological measurement, vol. 30, no. 7, p. 679, 2009. [PubMed: 19525570]

[27]. Inan OT et al., “Non-invasive cardiac output trending during exercise recovery on a bathroom-scale-based ballistocardiograph,” Physiological measurement, vol. 30, no. 3, p. 261, 2009. [PubMed: 19202234]

[28]. Inan OT et al., “Novel wearable seismocardiography and machine learning algorithms can assess clinical status of heart failure patients,” Circulation: Heart Failure, vol. 11, no. 1, p. e004313, 2018. [PubMed: 29330154]

[29]. Hernandez J. Bioglass: Physiological parameter estimation using a head-mounted wearable device; Proceedings of the 2014 4th International Conference on Wireless Mobile Communication and Healthcare - ”Transforming Healthcare Through Innovations in Mobile and Wireless Technologies”, MOBIHEALTH 2014; IEEE; 2014. 55–58.

[30]. Conn NJ et al., “In-Home Cardiovascular Monitoring System for Heart Failure: Comparative Study,” JMIR mHealth and uHealth, vol. 7, p. e12419, 1 2019. [PubMed: 30664492]

[31]. Tanaka S. Fully Automatic System for Monitoring Blood Pressure from a Toilet-Seat Using the Volume-Oscillometric Method; 2005 IEEE Engineering in Medicine and Biology 27th Annual Conference; IEEE; 2005. 3939–3941.

[32]. Etemadi M. Tracking clinical status for heart failure patients using ballistocardiography and electrocardiography signal features; Engineering in Medicine and Biology Society (EMBC), 2014 36th Annual International Conference of the IEEE; IEEE; 2014. 5188–5191.

[33]. Zile et al., “Effects of Exercise on Left Ventricular Systolic and Diastolic Properties in Patients With Heart Failure and a Preserved Ejection Fraction Versus Heart Failure and a Reduced Ejection Fraction,” Circulation: Heart Failure, vol. 6, pp. 508–516, 5 2013. [PubMed: 23515277]

[34]. Van Aelst LN et al., “Acutely decompensated heart failure with preserved and reduced ejection fraction present with comparable haemodynamic congestion,” European Journal of Heart Failure, vol. 20, pp. 738–747, 4 2018. [PubMed: 29251818]

[35]. Inan OT et al., “Noninvasive measurement of physiological signals on a modified home bathroom scale,” IEEE Transactions on Biomedical Engineering, vol. 59, no. 8, pp. 2137–2143, 2012. [PubMed: 22318479]

[36]. Inan OT et al., “Novel methods for estimating the ballistocardiogram signal using a simultaneously acquired electrocardiogram,” in Engineering in Medicine and Biology Society, 2009., pp. 5334–5347, IEEE, 2009.

[37]. Pan J and Tompkins WJ, “A real-time QRS detection algorithm,” IEEE Trans. Biomed. Eng, vol. 32, no. 3, pp. 230–236, 1985. [PubMed: 3997178]

[38]. Martínez A. A new method for automatic delineation of ECG fiducial points based on the Phasor Transform; Engineering in Medicine and Biology Society (EMBC), 2010 Annual International Conference of the IEEE; IEEE; 2010. 4586–4589.

[39]. Goldberger AL et al., “PhysioBank, PhysioToolkit, and PhysioNet: Components of a New Research Resource for Complex Physiologic Signals,” Circulation, vol. 101, no. 23, pp. e215–e220, 2000 (6 13). Circulation Electronic Pages: http://circ.ahajournals.org/content/101/23/e215.full doi: 10.1161/01.CIR.101.23.e215. [PubMed: 10851218]

[40]. Javaid AQQ, Multi-sensor signal processing methods for home monitoring of cardiovascular and respiratory diseases. PhD thesis, Georgia Institute of Technology, 2016.

[41]. Inan OT et al., “Ballistocardiography and seismocardiography: a review of recent advances.,” IEEE J. Biomedical and Health Informatics, vol. 19, no. 4, pp. 1414–1427, 2015.

[42]. Zhang H. Towards precise tracking of electric-mechanical cardiac time intervals through joint ECG and BCG sensing and signal processing; Engineering in Medicine and Biology Society (EMBC), 2017 39th Annual International Conference of the IEEE; IEEE; 2017. 751–754.

[43]. Pino EJ et al., “BCG algorithm for unobtrusive heart rate monitoring,” in Healthcare Innovations and Point of Care Technologies (HI-POCT), 2017 IEEE, pp. 180–183, IEEE, 2017.

[44]. Bruser C et al., “Automatic detection of atrial fibrillation in cardiac vibration signals,” IEEE Journal of Biomedical and health informatics, vol. 17, no. 1, pp. 162–171, 2013. [PubMed: 23086532]

[45]. Wiens A. Wearable ballistocardiography: Preliminary methods for mapping surface vibration measurements to whole body forces; Engineering in Medicine and Biology Society (EMBC), 2014 36th Annual International Conference of the IEEE; IEEE; 2014. 5172–5175.

[46]. Etemadi M et al., “Rapid assessment of cardiac contractility on a home bathroom scale,” IEEE Transactions on Information Technology in Biomedicine, vol. 15, no. 6, p. 864, 2011. [PubMed: 21843998]

[47]. Ashouri H et al., “Unobtrusive estimation of cardiac contractility and stroke volume changes using ballistocardiogram measurements on a high bandwidth force plate,” Sensors, vol. 16, no. 6, p. 787, 2016.

[48]. Giovangrandi L. Preliminary results from BCG and ECG measurements in the heart failure clinic; Engineering in Medicine and Biology Society (EMBC), 2012 Annual International Conference of the IEEE; IEEE; 2012. 3780–3783.

[49]. Chang Y-W and Lin C-J, “Feature ranking using linear SVM,” in Causation and Prediction Challenge, pp. 53–64, 2008.

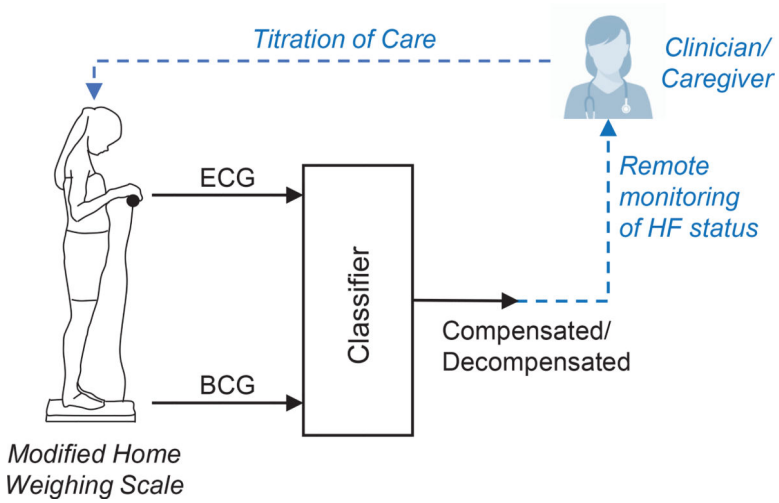

Fig. 1.

Illustration of our envisioned three-step solution for sensor-enabled maintenance of compensation in HF. 1) Recording of BCG and ECG signals at home using a modified weighing scale. 2) Classification of recordings to predict the clinical state of HF (compensated/ decompensated). 3) Intervention by a clinician based on the remote assessment of HF status.(Future work)

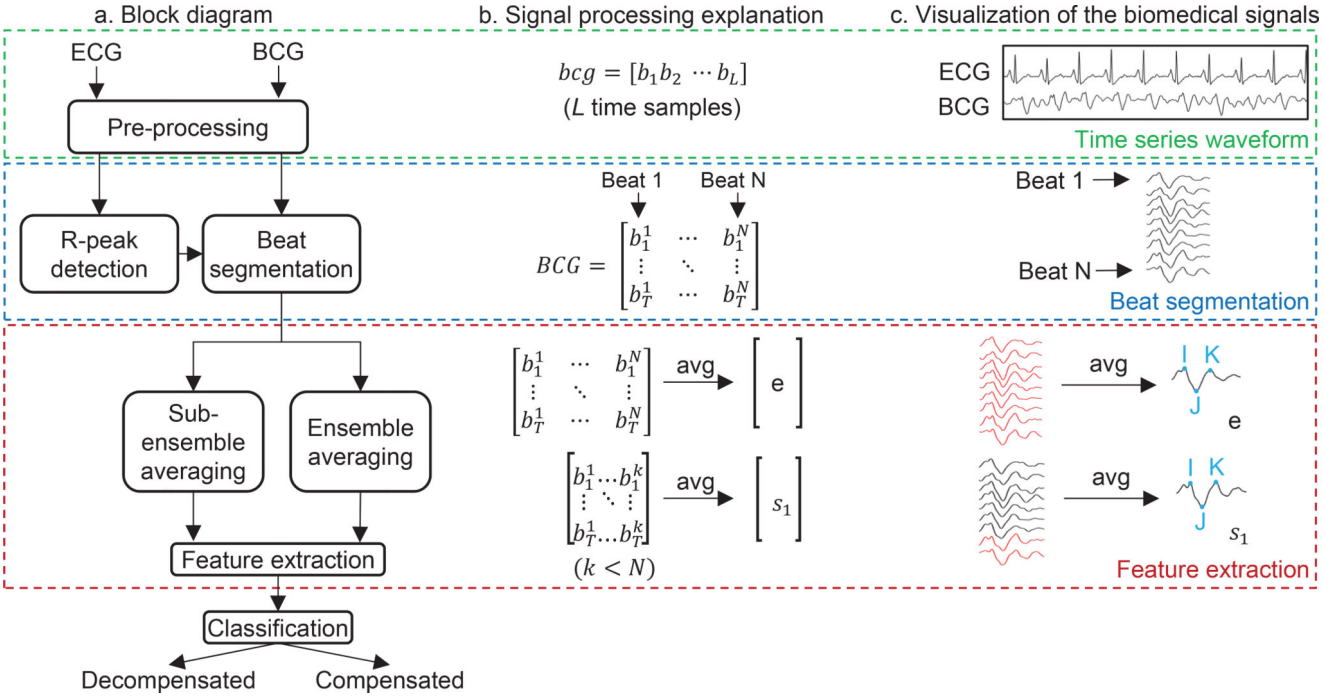

Fig. 2.

Steps involved in the process of classification into compensated and decompensated states. The process can be grouped into three broad stages: Obtaining a time series waveform, beat segmentation, feature extraction and classification. (a) Block diagram illustrating the steps within each stage. (b) Mathematical explanation of each stage with a representative BCG vector. (c) Illustration of each step with exemplary biomedical signals.

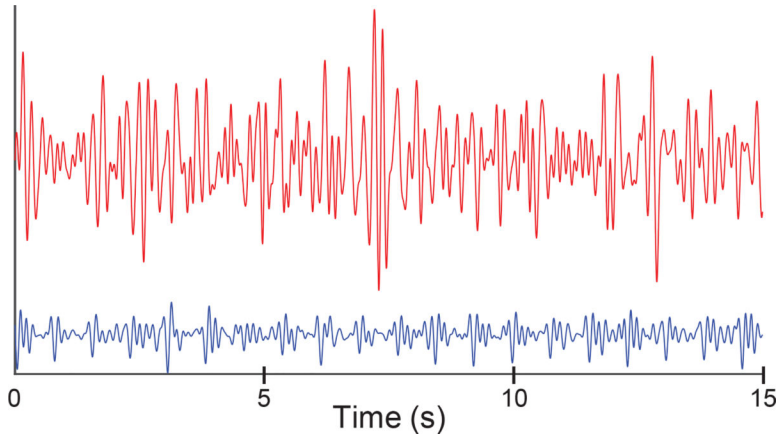

Fig. 3.

Example of two BCG signals collected; the signal in blue is a high-quality recording obtained while the signal in red is a low-quality recording. The ML estimate of SNR value for the two signals is 23.685 and 0.2844 respectively.

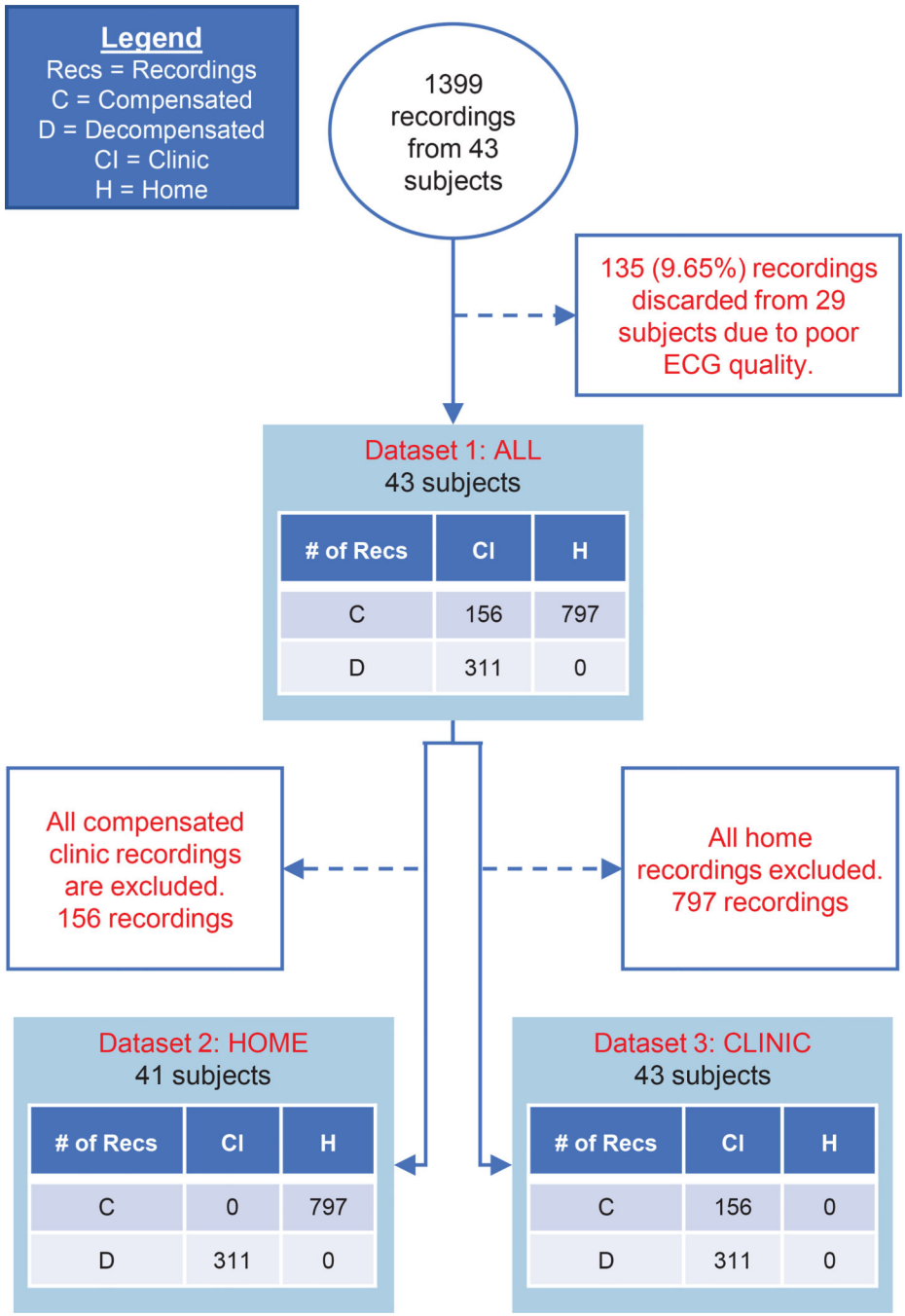

Fig. 4.

Illustration of selection of recordings for each of our three datasets along with exclusion criteria. White boxes show exclusion criteria, blue boxes show distribution of recordings between the home and clinic settings and compensated/decompensated patient status (see figure legend for details). Dataset 1 uses all recordings and tests the ability to discriminate between compensated and decompensated states under both recording conditions. Dataset 2 includes compensated home recordings and decompensated clinical recordings. Dataset 3

has only clinical data. Datasets 2 and 3 are constructed to assess any differences in performance between the home and clinic settings.

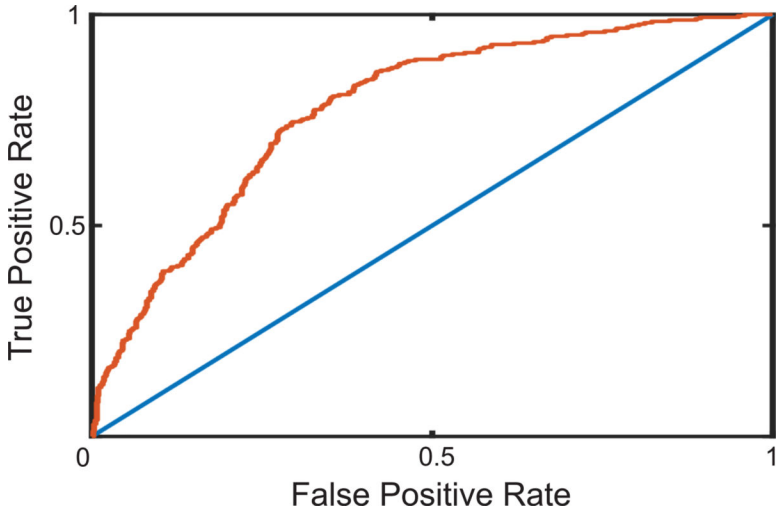

Fig. 5.

The red curve is the Receiver Operating Characteristic (ROC) curve of the best performing classifier - SVM with RBF kernel. The blue line is the ROC curve classification based on random chance. The area under the ROC curve value is 0.78. Result is using Dataset 1 (1264 recordings).

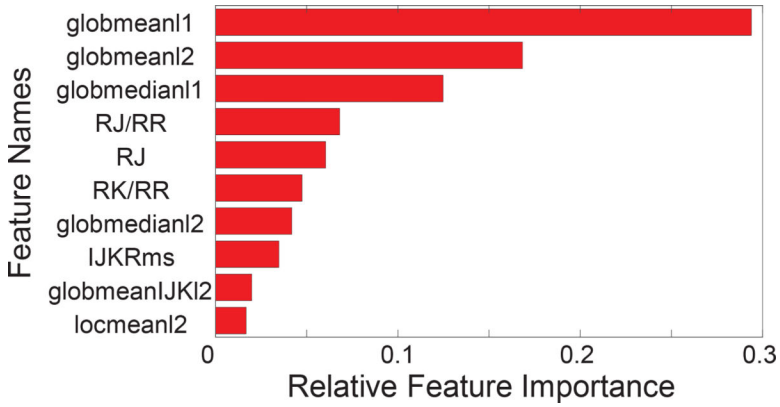

Fig. 6.

The ten most important features for this classification task arranged in the decreasing order of feature importance. The the bar plot indicates the relative value of feature importance obtained from the linear SVM weights.

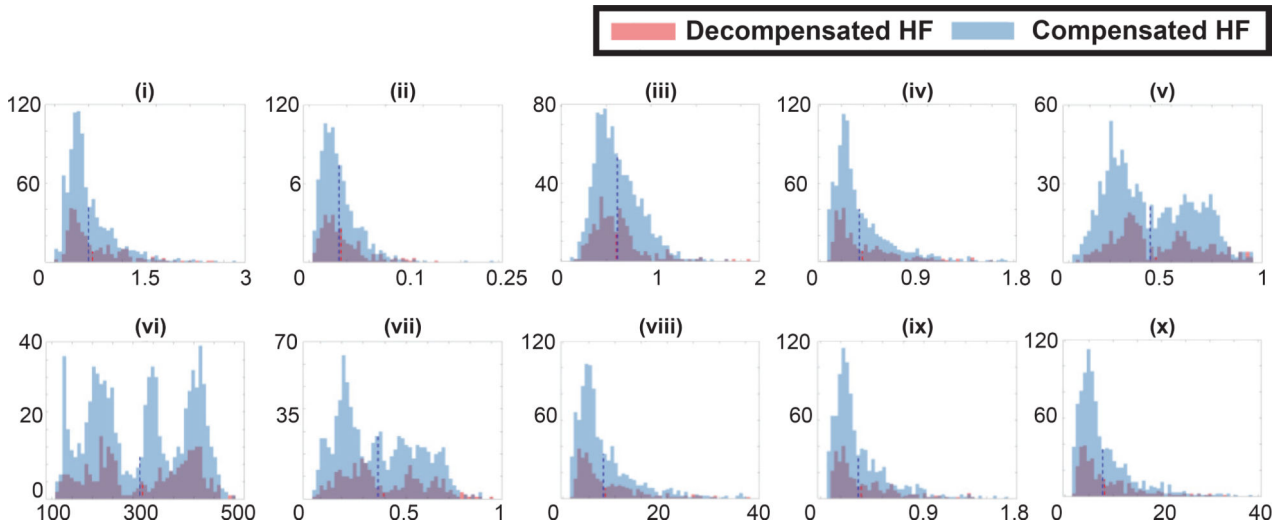

Fig. 7.

Each plot shown is a histogram of one feature over the compensated and decompensated classes. Plots (i) - (x) correspond to the features listed in Figure 6 in the increasing order of feature importance.

TABLE I

Demographic information of subjects

	Gender		NYHA Class			Overall
	Male	**Female**	**I**	**II**	**III-IV**	
# Patients	37	6	5	10	28	43
# Inpatient Recordings	434	26	16	60	384	460
# Outpatient Recordings	645	294	205	344	390	939
# Comp. Recordings	738	305	205	364	474	1043
# Decomp. Recordings	341	15	16	40	300	356
Age ($\mu \pm \sigma$)	60.2 12.9	52.5 10.2	65.2 6.2	55.0 15.7	59.5 12.3	59.1 12.7
Height ($\mu \pm \sigma$, in cm)	179.5 9.2	165.1 8.6	171.2 9.6	180.1 6.9	177.7 11.3	177.5 10.4
BMI ($\mu \pm \sigma$, in kg/m^2)	27.4 6.9	25.3 6.5	23.1 4.9	31.6 5.9	25.5 6.6	26.9 6.9

TABLE II

Ensemble Averaged Beat Features

Feature Name	Description	Feature Name	Description
RI	RI time interval	IJ_{Amp}	Amplitude of IJ
RJ	RJ time interval	IJK_{RMS}	RMS value of the IJK
RK	RK time interval	JAmpHR	Amplitude of J×Heart Rate
IK	IK time interval	RK/RR interval	RK /mean RR interval
IJK_{RMS}/RR interval	RMS value of IJK/mean RR interval	RI/RR interval	RI /mean RR interval
RJ/RR interval	RJ /mean RR interval		

TABLE III

Waveform Consistency Features

Feature Name	Description
$\text{global}\begin{Bmatrix}\text{mean}\\ \text{median}\\ \text{std}\end{Bmatrix}\text{L2}$	L2 distance between sub-ensemble averages and ensemble averages.
$\text{local}\begin{Bmatrix}\text{mean}\\ \text{median}\\ \text{std}\end{Bmatrix}\text{L2}$	L2 distance between sub-ensemble average pairs.
$\text{global}\begin{Bmatrix}\text{mean}\\ \text{median}\\ \text{std}\end{Bmatrix}\text{L1}$	L1 distance between sub-ensemble averages and ensemble averages.
$\text{local}\begin{Bmatrix}\text{mean}\\ \text{median}\\ \text{std}\end{Bmatrix}\text{L1}$	L1 distance between sub-ensemble average pairs.
$\text{global IJK}\begin{Bmatrix}\text{mean}\\ \text{median}\\ \text{std}\end{Bmatrix}\text{L2}$	L2 distance between IJK parts of sub-ensemble and ensemble averages.
$\text{local IJK}\begin{Bmatrix}\text{mean}\\ \text{median}\\ \text{std}\end{Bmatrix}\text{L2}$	L2 distance between IJK parts of sub-ensemble average pairs.
$\text{global CCoef}\begin{Bmatrix}\text{mean}\\ \text{median}\\ \text{std}\end{Bmatrix}$	Correlation coefficient between sub-ensemble averages and ensemble averages.
$\text{local CCoef}\begin{Bmatrix}\text{mean}\\ \text{median}\\ \text{std}\end{Bmatrix}$	Correlation coefficient between sub-ensemble average pairs.

TABLE IV

Miscellaneous Features

Feature Name	Description
weight	DC component of the BCG signal
mean, median, std, 1st quartile, 3rd quartile (IJ)	Statistics of IJ amplitude from each BCG beat obtained using timing intervals from the ensemble averaged beats.
mean, median, std, 1st quartile, 3rd quartile (IJK_{RMS})	Statistics of RMS value of IJK from each BCG beat obtained using timing intervals from the ensemble averaged beats.
SNR, stdSNR	SNR and standard deviation instead of mean in equation 6.

TABLE V

AUC scores of classifiers performing LOSO cross validation on Dataset 1. Each result is from 1264 recordings.

	RF	Linear SVM	Polynomial SVM	RBF SVM	MLP
AUC	0.674	0.682	0.759	0.778	0.752

TABLE VI

Drop in AUC when the top 5 features from figure 6 are removed (dataset 1). Each result is from 1264 recordings.

	Remove glob meanl2	Remove RJ/RR	Remove RJ	Remove glob meanl1	Remove glob medianl1
Drop in AUC (RBF SVM)	0.086	0.058	0.048	0.047	0.047

TABLE VII

AUC score obtained under the two experimental settings: clinic and home.

	AUC (RBF SVM)	Number of LOSO folds	Number of Recordings
Clinic	0.605	28	467
Home	0.667	18	1108